Molecular Crystals and Liquid Crystals

Publication details, including instructions for authors and subscription information:
http://www.tandfonline.com/loi/gmcl20

Crystallization Kinetics Study in Orthogonal Liquid Crystalline Phases Formed by Schiff's Base nO.m Compounds by Calorimetric and Dielectric Techniques - Part 2

T. Chitravel [a], M. L. N. Madhu Mohan [b] & V. Krishnakumar [c]

[a] Department Physical Sciences, Bannari Amman Institute of Technology, Sathyamangalam, India

[b] Liquid Crystal Research Laboratory, Bannari Amman Institute of Technology, Sathyamangalam, India

[c] Department of Physics, Periyar University, Salem, India

Version of record first published: 17 Dec 2009

To cite this article: T. Chitravel, M. L. N. Madhu Mohan & V. Krishnakumar (2009): Crystallization Kinetics Study in Orthogonal Liquid Crystalline Phases Formed by Schiff's Base nO.m Compounds by Calorimetric and Dielectric Techniques - Part 2, Molecular Crystals and Liquid Crystals, 515:1, 49-63

To link to this article: http://dx.doi.org/10.1080/15421400903290691

Mol. Cryst. Liq. Cryst., Vol. 515, pp. 49–63, 2009

ISSN: 1542-1406 print/1563-5287 online
DOI: 10.1080/15421400903290691

Crystallization Kinetics Study in Orthogonal Liquid Crystalline Phases Formed by Schiff's Base nO.m Compounds by Calorimetric and Dielectric Techniques – Part 2

T. Chitravel[1], M. L. N. Madhu Mohan[2], and V. Krishnakumar[3]
[1]Department Physical Sciences, Bannari Amman Institute of Technology, Sathyamangalam, India
[2]Liquid Crystal Research Laboratory, Bannari Amman Institute of Technology, Sathyamangalam, India
[3]Department of Physics, Periyar University, Salem, India

A systematic kinetic study of crystallization among two smectogens of higher homologues of the benzylidene aniline nO.m series viz. 4O.16 and 8O.16 has been carried out by thermal microscopy, differential scanning calorimetry (DSC), and dielectric studies. The crystallization kinetics was studied by two techniques, viz., the traditional thermal analysis (i.e., DSC) and dielectric studies, viz., permitivitty and dielectric loss variation with temperature. The DSC thermo grams were run from crystallization temperature to the isotropic melt for different time intervals. The liquid crystalline behavior together with the rate of crystallization of Smectic ordering in newly synthesized nO.m compounds were discussed in relation to the kinetophase (which occurs prior to the crystallization). The molecular mechanism and dimensionality in the crystal growth were computed from the Avrami equation. The characteristic crystallization time (t^*) at each crystallization temperature was deduced from the individual plots of log t and ΔH. Further, it was observed that the data obtained from DSC and dielectric studies were in good agreement with one another.

Keywords: crystallization kinetics; DSC; kinetophase; liquid crystals

1. INTRODUCTION

Liquid Crystals are those which exhibit anisotropic property of solids as well as fluidity of isotropic liquid and are made up of calamitic

Address correspondence to V. Krishnakumar, Department of Physics, Periyar University, Salem, India. E-mail: vkrishna_kumar@yahoo.com

molecules. The rod-like shaped molecules, which can be obtained by joining the two or more phenyl rings or cyclohexyl rings with a relatively rigid bridging group and attached with flexible aliphatic end-chains, when self-assembled into molecular organized structures with long range orientational order show anisotropy as well as fluidity as a function of temperature, and they are called liquid crystals [1]. The study of crystallization kinetics [2,3] is a powerful tool to understand the various mechanisms involved in the crystallization of liquid crystals.

The liquid crystalline materials belonging to the class of benzylidene aniline exhibits a fascinating mesomorphic behavior associated with a distinct molecular ordering; the convenient working thermal range makes them suitable for systematic kinetic investigations. In continuation of our experimental studies [4,5] on nO.m and ferroelectric liquid crystals, here we present a detailed analysis of two smectogens of higher homologues of the benzylidene aniline nO.m series, viz., 4O.16 and 8O.16.

2. EXPERIMENTAL

The nO.m compounds of the present investigation were synthesized and characterized as reported earlier [6]. The crystallization kinetics of the present compounds, determined by the rate of growth of a particular transition, were performed on a Shimadzu DSC-60 differential scanning calorimeter and Agilent 4192A LF impedance analyzer. The thermograms at each crystallization temperature, together with simultaneous phase identification [7], were obtained using a Instec Stand alone Temperature Controller (STC 200) supplemented by Nikon polarizing microscope equipped with digital camera (DS-U1) and associated software (ACT-2U). The differential scanning calorimetry (DSC) measurements were performed on each member of pure nO.m compounds (3–7 mg sample) using aluminum and/or glass crucibles. A typical DSC scan for a given sample at each crystallization temperature is described as follows. The sample was heated to its isotropic melt with a scan rate of 10°C min^{-1}; after holding for 1 min to attain thermal equilibrium, the sample was cooled at the same scan rate to its predetermined crystallization temperature. After holding for a requisite time interval at crystallization temperature, the endothermic peaks were recorded while the sample was cooled to the crystal state at of 10°C min^{-1}. This process was repeated for each individual member of the nO.m series at the appropriate preselected crystallization temperatures.

For the elicitation of the dielectric data, the nO.m sample under investigation was filled in a polyamide buffed cells (Instec Inc., USA) in its isotropic state under suction. Silver paste and wires were used

to draw the electrodes from the cell. The cell was placed in a Instec hot and cold stage (HCS402) equipped with Instec Stand alone Temperature Controller (STC 200). The temperature is monitor and controlled through a computer by a software program (Wintemp) to an accuracy of $\pm 0.01^{\circ}C$. The sample was heated to its isotropic melt with a scan rate of $10^{\circ}C\ min^{-1}$; after holding for a period of 1 min to attain thermal equilibrium, the sample was cooled at $0.5^{\circ}C\ min^{-1}$ scan rate to its predetermined crystallization temperature. After holding for a requisite time interval at crystallization temperature, the data of capacitance and dielectric loss were noted for each time interval. This process was repeated for each individual member of the nO.m series at the appropriate preselected crystallization temperatures.

2.1. Synthesis of the Compounds

The compounds were prepared [6,7] by condensation of the respective alkoxy benzaldehyde (0.1 mole) and alkyl aniline (0.1 mole) in refluxing in absolute ethanol in the presence of a few drops of glacial acetic acid. After refluxing the reactants for four hours, the solvent was removed by distillation under reduced pressure. The crude sample was subjected to repeated recrystallization from cold absolute ethanol, till transition temperatures were found to be reproducible.

The homologous series N-(p-n-alkoxybenzylidene)-p-alkylaniline are Schiff s bases with the general molecular formula is given below:

where n and m represent the number of carbon atoms in alkoxy and alkyl end-chains, respectively. The anilines used for the synthesis of the above compounds are obtained from Sigma Aldrich Chemicals while the alkoxybenzaldehydes were synthesized in our laboratory.

2.2. Synthesis of p-n-Butyl/octyloxybenzaldehyde

To a cyclohexanone solution containing p-hydroxybenzaldehyde (1.83 gm/15 mmol) and n-butyl bromide (2.7 ml/20 mmol), 5.15 gm/ n-octylbromide (3.8 ml/20 mmol), 5.15 gm of (37.5 mmol) of anhydrous potassium carbonate was added slowly with constant stirring. The reaction mixture was then heated under reflux for 3 hours until the evolution of CO_2 ceased. After cooling to room temperature, the reaction mixture was filtered off to remove excess of K_2CO_3 and KBr formed during the reaction. The precipitate was washed repeatedly with excess

of ether. On evaporation the excess ether and cyclohexanone under reduced pressure, a colorless oil product (75% yield) was obtained. The oil product was further purified by passing through a silica gel column using a mixture of benzene and acetone in the volume ratio 1:4.

3. RESULT AND DISCUSSION

3.1. Phase Identification

The observed phase variants, transition temperatures, and corresponding enthalpy values obtained by thermal microscopy, dielectric studies, and DSC are presented in Table 1. The compounds of the present nO.m series are found to exhibit characteristic textures [8], viz., focal-conic fan texture in Smectic A phase, the appearance of transient transition bars across focal-conic fans in the Smectic B phase. Nematic phase is identified by the figure print texture of Nematic droplets. The 4O.16 exhibits tri-variant phase sequence (NAB), while 8O.16 exhibits di-variant phase sequence (AB). The phase variance of the compounds in the cooling run from isotropic to crystal are depicted below:

4O.16 Isotropic → Nematic → Smectic A → Smectic B → Crystal

8O.16 Isotropic → Smectic A → Smectic B → Crystal.

Further, the phase transition temperatures observed by thermal microscopy are found to be in good agreement with those obtained from calorimetric and dielectric studies.

TABLE 1 Transition Temperatures (in°C) Obtained from Thermal Microscopy (TM), Differential Scanning Calorimetry (DSC), and Dielectric Studies of nO.m Compounds. Corresponding Enthalpy Values (in J/g) are Given in Parenthesis

				Dielectric studies	
nO.m	Phase transition	TM	DSC	Capacitance	Dielectric loss
8O.16	Iso – Sm A	86.1	85.70 (0.24)	86.2	86.1
	Sm A – SmB	65.9	65.83 (5.96)	66.2	66.1
	SmB – Crystal	44.7	43.68 (63.58)	44.8	44.9
4O.16	Iso – N	63.15	63.40 (9.10)	63.05	63
	N – Sm A	61.55	61.44 (*)	61.38	61.38
	SmA – Sm B	54.21	54.15 (2.81)	54.10	54.15
	Sm B – Crystal	50.16	50.18 (50.36)	50.12	50.14

*Not properly resolved.

3.2. Selection of Thermal Range of Crystallization Temperatures

The procedure for the thermal selectivity for the crystallization temperatures (CT) is described for 80.16 as a representative member of the present work. The DSC thermograms of the 80.16 is illustrated in Fig. 1. In the heating run, the 8O.16 mesogen melts at 67.95°C with an enthalpy value of 82.55 J/g to the Smectic B phase, the Smectic B to Smectic A transition is observed at 76.90°C with an enthalpy value of 5.15 J/g, while the Smectic A to isotropic is found to be 85.05°C with an enthalpy value of 0.37 J/g. The compounds exhibit three distinct transition in the cooling run at 85.70°C, 65.83°C, and 43.68°C, with heat of transition 0.24 J/g, 5.96 J/g, and 63.58 J/g, respectively. From this data it is inferred that the thermal span of mesomorphic phase as $(T_{Iso\text{-}A},) - (T_{SmB\text{-}Cry})$ is 42°C. Once the $T_{SmA\text{-}SmB}$ is completed, the kinetics of crystallization from Smectic B could be investigated over a temperature range between $T_{SmA\text{-}SmB}$ and $T_{SmB\text{-}Cry}$, provided the crystallization kinetics are not too fast.

A kineto phase is defined as the phase that occurs prior the crystallization. To be precise, in the present context, for 8O.16 the phase sequence is Iso – Sm A – Sm B – Crt. Hence Smectic B is referred as the kineto phase. Similarly, in 4O.16 mesogen the phase sequence is Iso – Nematic – Sm A – Sm B – Crt. In this case also Smectic B is referred

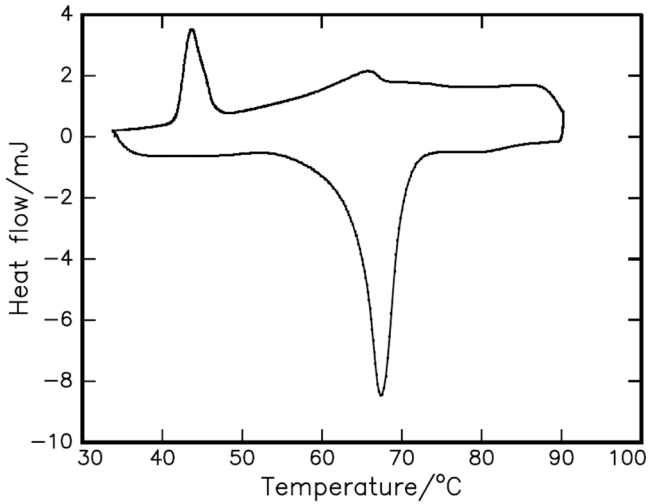

FIGURE 1 DSC heating and cooling thermograms of 80.16 recorded at a scan rate of 10°C min^{-1}.

as the kineto phase. Hence in both the mesogens, viz., 8O.16 and 4O.16, the phase Smectic B is referred as a kineto phase.

3.3. Crystallization Kinetics through DSC

The crystallization kinetics of 8O.16 relating to the phase transition from Smectic B to the melt is selectively performed at each predetermined crystallization temperatures, viz., 51, 56, and 62°C. The sample is held at 51°C for different time intervals (0.1 to 7 min.). The heating curve with a crystallization time of $t = 0$ min is recorded immediately following the quenching from the melt to the crystal, at crystallization temperature 51°C. This curve displays only Smectic A to isotropic endoderm indicating that the Smectic B to Smectic A transition has not yet occurred. However, in small increments of time, at $t = 0.1$ min, the appearance of a small peak is attributed to a Smectic B to Smectic A transition suggesting fast crystallization.

The enthalpy values for individual transitions at different time intervals are calculated at each crystallization temperature, and the corresponding data plotted against the corresponding logarithm of time intervals for each member of n.Om series. Figure 2 shows plots for crystallization of the 8O.16 compound at 51°C. and 56°C. These plots have an identical shape, apart from the shift in the log t axis, suggesting the limitations of the rate of crystallization kinetics [10].

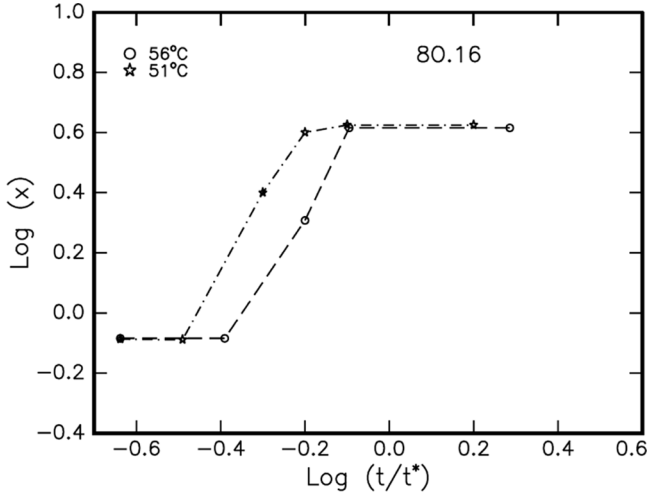

FIGURE 2 Heats of melting as a function of logarithm of annealing time in the Smectic B of 8O.16 at 51°C and 56°C.

A plot of heats of melting of the mesomorphic phase, viz., the log of annealing time for different crystallization temperatures of the 8O.16 obtained by shifting data along the log t axis to the 56°C curve is depicted in Fig. 3. Such a master curve strongly suggests that the same mechanism operates for crystallization in the Smectic A and Smectic B phases. Super cooling is understood as a state where lack of any proper nucleus. The liquid phase can be maintained all the way down to the temperature at which crystal homogenous nucleation occurs. As expected [9], the overall crystallization rate is controlled by a nucleation rate influencing the rate of growth of domains. This is a function of the degree of super cooling and the starting Smectic mesophase.

Similar experimental studies are carried out for measurement of crystallization kinetics of the other compound (4O.16). The corresponding data of crystallization time t^* along with the calculated crystal growth parameters for different crystallization temperatures are summarized in Table 2, which includes the results relevant to the following sections.

3.4. Crystallization Kinetics through Dielectric Studies

It was earlier proposed by us [5] that the crystallization kinetics can also be studied and analyzed at a selected frequency with the dielectric

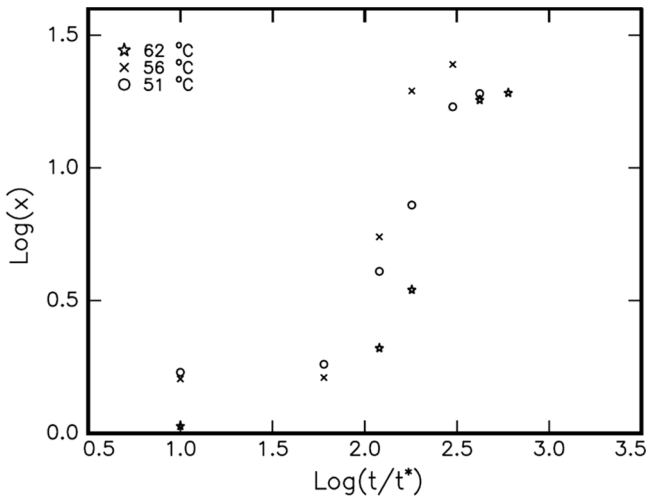

FIGURE 3 Plot of heats of melting of the mesomorphic phase of 8O.16 viz. the log of the annealing time for different temperatures, obtained by shifting data along the log t axis to the 56°C.

TABLE 2 Measured Crystallization Parameters for 63.2% Transformation from the Various Smectic Mesophases to the Crystalline Phase of nO.m Compounds Experimentally Obtained by Thermal and Electrical Studies

		Thermal studies			Electrical studies					
					Dielectric studies (1 KHz)					
		Differential scanning calorimetry (ΔH)			Permittivity (ε')			Dielectric loss (ε'')		
nO.m	CT/°C	t^*/sec	n	b	t^*/sec	n	b	t^*/sec	n	b
4O.16	52	87.49	0.7743	0.313×10^{-1}	386.1	0.4949	0.522×10^{-1}	333.92	0.4682	0.658×10^{-1}
	53	156.94	0.8373	0.145×10^{-1}	333.89	0.9107	0.503×10^{-2}	442.38	0.8522	0.556×10^{-1}
	54	157.17	1.2354	0.190×10^{-2}	258.69	0.6396	0.286×10^{-1}	180	0.3930	0.129×10^{-1}
8O.16	51	192.37	2.912	0.223×10^{-6}	100.53	0.573	0.712×10^{-1}	116.07	0.5517	0.728×10^{-1}
	56	142.82	2.317	0.101×10^{-4}	108.25	0.4118	0.145×10^{-1}	210.86	0.3762	0.133×10^{-1}
	62	272.6	1.232	0.990×10^{-3}	157.58	0.213	0.340	227.16	0.280	0.218

data. The crystallization kinetics relating to the phase transition from Smectic B to the melt of 8O.16 is selectively performed at each predetermined crystallization temperatures, viz., 51, 56, and 62°C at an excitation frequency of 1 KHz. The sample is held at 51°C for different time intervals (0.1 to 10 min). The dielectric data (capacitance and dielectric loss) at 1 KHz excitation frequency with a crystallization time of t = 0 to 10 min are recorded immediately following the quenching of the melt to crystal, at crystallization temperature 51°C. The capacitance and dielectric loss values for individual transitions at different time intervals are noted at each crystallization temperature, and the corresponding data plotted against the corresponding logarithm of time intervals for each member of n.Om series. Crystallization obtained by this technique of the 4O.16 compound at 52°C, 53°C, and 54°C are identical to those of DSC data curves suggesting the existence of the same mechanism in the rate of crystallization kinetics [4].

3.5. The Process of Crystallization

In general, the kinetics of crystallization involving the rate of growth of small domains in a smectic phase is manifested equally by its temperature and time. Temperature dependence of nucleation takes place as a homogenous process over a constant period of time. In addition, defects and impurities in the compound have a pronounced influence on the nucleation process [9]. Further, any impurity in the mesogen hampers the overall rate of phase transformation and the dimensional geometry of the growing domains.

It is well known that the crystallization process involving the fraction of the transformed volume x, at a time t, measured since the beginning of the crystallization process, is described by the Avrami equation [2,3]

$$x = 1 - \exp(-bt^n), \tag{1}$$

where the constants b and n depend on the nucleation mechanism and the dimensionality geometry of the growing domains, respectively. The transformed volume x at a crystallization time t is given by $\Delta H/\Delta H_o$, where ΔH is the crystal heat of melt measured at time t, and ΔH_o is the maximum value obtained from the plateau of the individual master curves (Fig. 3). A similar argument holds good for dielectric data $\Delta\varepsilon'/\Delta\varepsilon'_o$ and $\Delta\varepsilon'/\Delta\varepsilon''_o$, where $\Delta\varepsilon'$ and $\Delta\varepsilon''$ are the values of capacitance and dielectric loss at time t, and $\Delta\varepsilon'$, $\Delta\varepsilon''_o$ are the maximum value obtained from the plateau of the individual master curves.

If the kinetics of the crystallization from the corresponding smectic phases are described by the above Avrami equation; the data for all the crystallization temperatures can be applied to the single equation [9]

$$x = 1 - \exp[1 - (t/t^*)^n], \tag{2}$$

where $t^* = b^{-1/n}$. Further, the characteristic time t^* can be experimentally determined, since at $t = t^*$, $x = 0.632$. Substituting the values of t^* and x in Eq. (1), constants b and n are obtained at a specified crystallization temperature. It is found from the experimental data that the constant n, which manifests the dimensional geometry of the growing domains, is almost unaltered, while the magnitude of the constant b, which governs the nucleation mechanism, varies in the order of 10^{-1} to 10^{-6} for the compounds studied. The data of constants n and b experimentally obtained by calorimetric and dielectric studies (permittivity and dielectric loss) for various specified crystallization temperatures of 4O.16 and 8O.16 are tabulated in the Table 2.

For a specified crystallization temperature, the values of constants n and b are found to be unaltered in both thermal and electrical studies implying that the same type of nucleation mechanism is taking place in both nO.m compounds. The trend of the magnitude of the two constants n and b are found to be in agreement with the data reported for discotic [9] and smectic [4] mesophases. The variation of the magnitude of n in both nO.m compounds is attributed to the sporadic nucleation and growth in two dimensions.

3.6. Influence of Orthogonal Smectic B Phase Variant on Crystallization Kinetics

The phase sequence in liquid crystal molecules has a pronounced influence on their crystallization kinetics. The kineto phase, which occurs prior to the crystallization, is solely responsible for many combinational factors of the crystallization mechanism.

In the present study of 4O.16 and 8O.16 compounds, the kineto phase prior to crystallization is Smectic B. Our previous studies [4] on different nO.m compounds exhibiting various kineto phases concurred with data of the present investigations.

Further, in Smectic B, as expected, the rate of crystallization is rapid as it is close to the crystalline phase. It is a known fact that crystallization kinetics will be fast for the CT near to the homogenous nucleation temperature, and slow when the CT is near the isotropic melt.

3.7. Influence of Alkyloxy Carbons

Both 4O.16 and 8O.16 compounds have same kineto phase, Smectic B. The data from Table 1 suggest the liquid crystalline phase thermal range is 13°C and 42°C for 4O.16 and 8O.16 compounds, respectively. Further the kineto phase (Smectic B) thermal range is increased from ~3°C to ~22°C in both compounds with increase in alkyloxy carbon number; however, as expected, the isotropic clearing point shifts to higher temperature with increase in carbon chain length. It is evident from Table 2, that the degree of variation of dimensionality parameter n infer a unique crystallization mechanism for these compounds. A possible explanation for crystallization dimensionality is a sporadic nucleation and growth involving a homogenous process of continuous nucleation over a constant time [9]. Furthermore, the volume transformation calculated at individual c time t^* is in accordance with Eq. (2) which strongly implies the completion of the crystallization process.

3.8. Dielectric Studies

The dielectric studies allow to identify the phase transitions temperatures and the thermal range of individual phases. This study is a sophisticated tool to detect the second order transitions, which cannot be identified by DSC studies.

To calculate the leads capacitance, the liquid crystal cell is calibrated with a known (benzene) substance. Further, the empty liquid crystal cell is also calibrated against temperature in the range of 25°C to 150°C and with the frequency in the range of 100 Hz to 1 MHz, respectively. The compounds (4O.16 and 8O.16) are filled in a 4 micron spacer polyamide buffed cells (Instec, Inc., USA) in its isotropic state under sunction, the silver leads are drawn from to excite the cell with a frequency of 10 KHz and 100 KHz, respectively, obtained from an Agilent low frequency impedance analyzer (4192 A). This liquid crystal with compound is heated to its isotropic state and held for 10 min to attain thermal equilibrium. Further, it is cooled to crystal at a programmed scan rate of 0.1°C/min with an accuracy of ±0.01°C. This liquid crystal cell is placed in an Instec hot stage and is observed under crossed polars of a Nikon polarizing microscope. The simultaneous observation of the liquid crystal texture through polarizing microscope along with the dielectric data confirmed the formation and identification of the various smectic phases.

Compound 40.16 is chosen as a representative member of the present work and the plot of capacitance with temperature at two

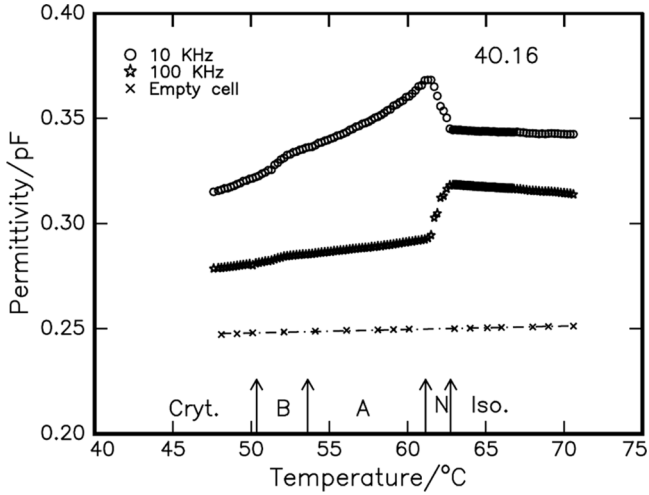

FIGURE 4 Temperature variation of permittivity at two frequencies (10 KHz and 100 KHz) identifying various liquid crystalline phases of 4O.16.

frequencies, viz., 10 KHz and 100 KHz, respectively, is depicted in Fig. 4. The corresponding dielectric loss for 100 KHz is illustrated in Fig. 5. The transition temperatures obtained from DSC, polarizing

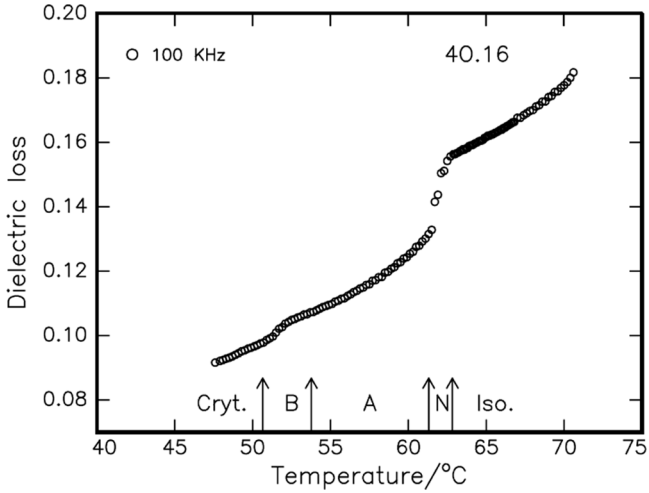

FIGURE 5 Temperature variation of dielectric loss at frequency 100 KHz identifying various liquid crystalline phases of 4O.16.

microscopic studies, and dielectrics studies are compared in Table 1. The following points are noted from Figs. 4 and 5:

a) The isotropic-to-nematic phase transition is manifested by a sudden jump at 63.05°C, which is observed in the 10 KHz and 100 KHz profiles of temperature variation of the permittivity indicating the starting of nematic phase. A similar trend of result is noticed in the dielectric loss profile also. Polarizing microscopic textural observation indicates isotropic-to-nematic transition occurred at 63.15°C, while DSC thermograms reveals this transition at 63.40°C, which concurred with the present dielectric studies. This transition is classified as first order because of the huge enthalpy value (6.53 J/g) obtained from DSC studies. Further, the sharp anomaly in the dielectric spectrum also testifies this.
b) The abrupt fall in the variation of the magnitudes of the permittivity and dielectric loss, with lowering of temperature to 61.38°C, is attributed to the phase transition from nematic to Smectic A phase. The same result is seen in permittivity and dielectric loss spectrum at two different frequencies. The simultaneous optical observation by polarizing microscope also confirms the onset of Smectic A phase at 61.55°C. DSC thermograms also indicate the onset of Smectic A phase at 61.4°C.
c) The thermal span of Smectic A phase is experimentally observed to be from 61.38°C to 54°C. A linear variation in the permittivity and dielectric loss spectrum indicates the stabilization of this phase.
d) At Smectic A to Smectic B transition, a small kink at 54.1°C in both profiles of dielectric spectrum indicates the growth of Smectic B phase. This transition is observed at 54.21°C from polarizing microscopic textural studies, which concurred with the dielectric result. It is noteworthy to mention that in the entire thermal range of this phase, except for linear variation of capacitance and dielectric loss, no anomaly is observed indicating the stabilization of the Smectic B phase.
e) At 50.12°C, a smooth variation in the dielectric profiles show the onset of the crystal. Simultaneous microscopic textural observation at the same temperature concurs with the data obtained from DSC and dielectric studies.

It is prudent to mention that in the present homologous series, the experimental results of the 4O.16 compound follow the same trend of the 8O.16 compound dielectric studies, as expected. These results are tabulated in Table 1. Furthermore, the transition temperatures obtained by various techniques, namely, dielectric studies, polarizing

microscopic textural observations, and DSC thermograms concur with each other as can be seen from Table 1.

CONCLUSIONS

1. In orthogonal ordering (Smectic B phase) the formation of an ordered domain occurs, which converts to a stable nucleus that initiates the aggregation of the surrounding molecules to form layered domains. The origin of this nucleus is critical since its formation proceeds until it reaches a sufficient size to initiate the crystallization process.
2. We propose that this process of crystallization is controlled by either the lamellar or interlayer distances in nontilted (Smectic B) kineto phase. In such a process of seed nucleation, factors relating to the smectic layer plays an important role. A particular molecule in the lower smectic layer first acquires the requisite energy to allow the formation of ordered domains, which in turn propagate crystallization to the adjacent smectic layers. These ordered domains will further proceed through the smectic layers by a process of successive addition of the molecules from neighboring layers leading to sporadic nucleation and growth in two dimensions. This process continues until the crystallization is completed.

ACKNOWLEDGMENTS

The authors thank the Management of Bannari Amman Institute of Technology for providing the laboratory and other infrastructural facilities. One of the authors (MLNMM), acknowledges the financial support provided by Department of Science and Technology, New Delhi, All India Council of Technical Education, New Delhi, and Defence Research Development Organization, New Delhi.

REFERENCES

[1] Demus, D. (1994). *Liquid Crystals: Phase Types Structures and Chemistry of Liquid Crystals*, Springer: New York.
[2] Avrami, M. (1939). *J. Chem. Phys.*, *7*, 1103.
[3] Avrami, M. (1940). *J. Chem. Phys.*, *8*, 212.
[4] Madhu Mohan, M. L. N., Arunachalam, B., & Aravind Sankar, C. R. (2008). *Met. Mat. Trans. A.*, *39*, 1192; Madhu Mohan, M. L. N., & Arunachalam, B. (2008). *Z. Naturforch*, *63a*, 435; Chitravel, T., Madhu Mohan, M. L. N., & Krishnakumar, V. (2008). (submitted to *Physica B Condensed Matter*); Kumar, P. A., Madhu Mohan, M. L. N., & Pisipati, V. G. K. M. (2000). *Liq. Cryst.*, *27*, 727;

Chitravel, T., Madhu Mohan, M. L. N., & Krishnakumar, V. (2008). *Mol. Cryst. Liq. Cryst.*, *493*, 17.
[5] Madhu Mohan, M. L. N. (2009). *Romanina J. Phys.* (in press).
[6] Pisipati, V. G. K. M., Rao, N. V. S., Padmaja Rani, G., & Bhaskara Rao, P. (1991). *Mol. Cryst. Liq. Cryst.*, *210*, 165.
[7] Keller, P., & Scheurle, B. (1969). *Angew Chem. Int. Ed. Engl.*, *8*, 884.
[8] Gray, G. W., & Goodby, J. W. G. (1984). *Smectic Liquid Crystals – Textures and Structures*, Leonard Hill: London.
[9] Pisipati, V. G. K. M., George, A. K., Srinivasu, Ch., & Murty, P. N. (2002). *Z. Naturforsch, 58a*, 103.
[10] Ziru, H., Yue, Z., & Caille, A. (1997). *Liq. Cryst.*, *23*, 317.